Estimating formation shear attenuation from frequency-dependent dipole-flexural wave attenuation

Qiaomu Qi, NUS; Arthur C. H. Cheng, NUS; Yunyue Elita Li, NUS*

SUMMARY

A key characteristic of dipole-flexural wave is that it travels with the formation shear slowness at the low frequency limit. In this work, we extend the workflow of extracting shear slowness from flexural wave dispersion to include the estimation of shear attenuation. The new workflow includes: 1. computing frequency-dependent flexural wave attenuation from array dipole data; 2. determining a characteristic frequency band where shear wave is dominant based on slowness probability; 3. averaging the flexural wave attenuation within the calibrated low frequency band to obtain the formation shear attenuation. In the synthetic example, the estimated shear attenuation is within 1% of the actual value. Application of the method to real data acquired in open borehole also produces reasonable results. Our work suggests that accounting for the frequency-dependency of flexural wave attenuation is crucial for an accurate formation shear attenuation estimate. With appropriate modification, the developed workflow is also applicable to frequency-dependent attenuation analysis for other borehole guided wave modes.

INTRODUCTION

Attenuation estimated from full waveform sonic logs provides in-situ information about the formation rock and fluid properties (Cheng et al., 1982). It finds important applications in many aspects such as, evaluating reservoir gas potential (Qi et al., 2017), aiding waveform inversion for providing realistic earth materials (Li et al., 2015) and calibrating rock physics model for reservoir characterization. Continuing efforts are being made to develop robust methods for enabling sonic attenuation in routine log interpretation.

The formation compressional wave attenuation is usually estimated from monopole waveforms by spectral ratio or centroid frequency shift methods (Cheng et al., 1982; Quan and Harris, 1997) applied to the earliest part of the P-wave arrivals. With an appropriate correction for the geometrical spreading, the monopole compressional wave attenuation estimate is often close to its actual value (Tang and Cheng, 2004). However, in most fast formation situations, the shear head wave is contaminated by the high amplitude pseudo-Rayleigh wave arrivals. While in slow formation (that is, formation shear slowness greater than the borehole mud slowness), neither shear head wave nor pseudo-Rayleigh waves are generated and estimating shear wave attenuation becomes even impossible.

A more reliable way for accessing shear wave attenuation is to use dipole measurements. A dipole source primarily excites flexural waves along with compressional and shear head waves. A key characteristic of flexural wave is that it propagates at formation shear and Stoneley-wave slowness at low and high frequencies respectively (Schmitt, 1988; Tang and Cheng, 2004). Another advantage of extracting shear wave attenuation from dipole is that the flexural wave is a surface-guided wave meaning it is free from geometrical spreading. Unlike monopole shear head wave, the flexural wave can be strongly dispersive in particular fast formation. This implies the corresponding attenuation would be also frequency dependent due to the geometry of the borehole. Most of the existing attenuation extraction methods (Cheng et al., 1982; Quan and Harris, 1997) which have a constant-Q assumption would not be applicable in this case.

In this work, we introduce a characteristic band approach for formation shear attenuation estimate from dipole waveforms. The method employs a low frequency band calibrated from the shear slowness probability to characterize the shear attenuation from the frequency-dependent flexural attenuation. We discuss the potential applications of the frequency-dependent attenuation analysis to other borehole guided waves.

ESTIMATE FREQUENCY-DEPENDENT ATTENUATION FROM ARRAY SONIC DATA

A sonic logging tool generally consists of transmitter section including monopole, dipole sources and a array of receivers. By firing the sources successively, the receivers record a series of waveforms at each depth. The amplitude spectrum of the borehole guided waves recorded by the ith receiver can be written as

$$X_i(\omega) = S(\omega)R(\omega)C(\omega)e^{-\alpha(\omega)(d+(i-1)\Delta d)}\,, \qquad (1)$$

where $S(\omega)$, $R(\omega)$ are the source and receiver functions, respectively. $C(\omega)$ incorporates the source and receiver coupling functions. d is the distance between the source and the first receiver. For borehole guided waves, there is no geometrical spreading term in eq. (1). The fact that borehole guided waves are free from geometrical spreading greatly simplifies our attenuation estimate procedure. By taking natural logarithm on both sides of eq. (1), rearranging and considering an array of receivers, we can express eq. (1) in the following vector form

$$\begin{bmatrix} \ln X_1(\omega) \\ \ln X_2(\omega) \\ \vdots \\ \ln X_i(\omega) \end{bmatrix} = -\alpha(\omega) \begin{bmatrix} 0 \\ \Delta d \\ \vdots \\ (i-1)\Delta d \end{bmatrix} + T(\omega)\,, \qquad (2)$$

where

$$T(\omega) = \ln S(\omega)R(\omega)C(\omega) - \alpha(\omega)d\,. \qquad (3)$$

We assume the function $T(\omega)$ is independent of the relative travel distances $(i-1)\Delta d$ since geometrical spreading does not apply to guided waves. Then, Eq. (2) shows the log amplitude spectra is linearly proportional to the relative travel distance and the proportional coefficient is the negative attenuation coefficient. Thus, by fitting a straight line of the log amplitude spectra as a function of the relative travel distance, we can obtain the attenuation coefficient by finding the corresponding

slope. We repeat the same procedure for each frequency and calculate the frequency-dependent attenuation coefficient. A more common measure of the attenuation is the inverse quality factor which can be expressed as

$$\frac{1}{Q(\omega)} = \frac{2}{\omega}\frac{\alpha(\omega)}{p(\omega)}, \tag{4}$$

where $p(\omega)$ is the frequency-dependent slowness, which can be computed using the weighted spectral semblance method (Nolte et al., 1997). Borehole guided wave is dispersive due to the geometry of the borehole. This is the main reason that the attenuation coefficient or the inverse quality factor of borehole guided wave is frequency-dependent.

APPLICATION TO DIPOLE-FLEXURAL WAVE

We proceed with preparing synthetic array sonic data for calculating the frequency-dependent attenuation. We employ the frequency-wavenumber integration method (Cheng et al., 1982; Schmitt, 1988) to simulate the waveforms generated by a dipole source. The attenuation effect is taken into account by using complex velocities calculated from the constant-Q model. We assume the sonic logging tool consists of 1 dipole source and 8 receivers. The distance between the source and the first receiver is 3.56 m (140 inch) and the receiver spacing is 0.1524 m (0.5 ft). A minimum phase wavelet of 3 kHz center frequency is used as the source wavelet. Other relevant parameters are $V_p = 3800$ m/s, $V_s = 2350$ m/s, $V_f = 1500$ m/s, $\rho_b = 2434$ g/cm^3, $\rho_f = 1000$ g/cm^3, $Q_p = 100$, $Q_f = 300$ and 20 cm as borehole diameter. The individual waveform contains a total of 512 time samples. The fast Fourier transform (FFT) is applied to obtain the amplitude and phase spectra of the waveforms. To have a densely sampled spectra, the time series are padded to eight times of its original length before the FFT. The resulting slowness dispersion and attenuation of the flexural wave are plotted in Figure 1(a) and Figure 2. In Figure 2, the circles, squares, triangles, dots and diamonds correspond to a shear wave quality factor of 15, 20, 25, 30, 35. It is evident from Figure 2, the attenuation monotonically increases as the frequency decreases. This is explained by the fact that flexural wave attenuation approaches to mud and shear attenuation at high and low frequency limits. The flexural wave attenuation starts to flatten and fluctuates around the formation shear attenuation (donoted by the dashed line) when the frequency is below 4 kHz.

SHEAR ATTENUATION ESTIMATE: A CHARACTERISTIC BAND APPROACH

Theoretically, we can track the frequency-dependent attenuation at their low frequency asymptotes to obtain the shear attenuation. However, in practice, this is not usually a trivial task as the amplitudes of the waveform tend to be very small at low frequencies. Because in dipole measurements, the peak excitation frequency is generally much larger than the frequency band where shear wave prevails. At the low frequency limit, the amplitude decay between successive receivers is if

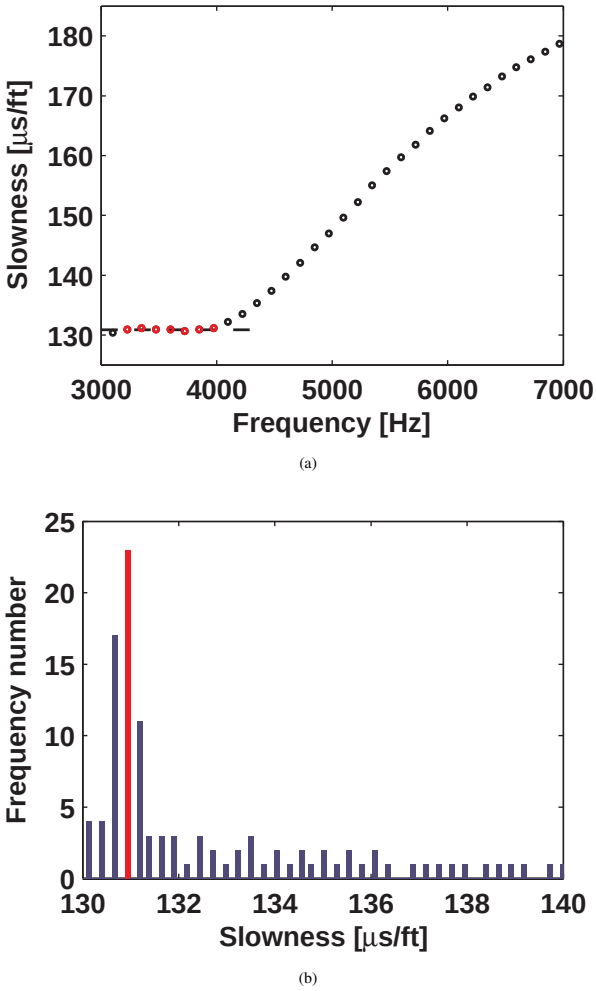

Figure 1: Synthetic data example: (a) slowness dispersion curve;(b) slowness probability histogram.

not completely but close to indistinguishable. In this case, the calculation of attenuation is very much prone to noises. However, comparing to the amplitude, the phase spectra is more stable at the low frequencies. As evidenced by comparing Figure 2 and Figure 1(a), the flat portion of the slowness is more prominent than in the attenuation. A key assumption that can be made here is, at the finite frequency band where the flat feature occurs in the flexural wave slowness dispersion, the wave experiences shear attenuation and travels at the formation shear slowness. With this, we introduce a more practical way of deducing shear attenuation from flexural wave attenuation.

In the first step, we apply the automatic pattern recognition technique (Huang and Yin, 2005) for picking the formation shear slowness. Based on the slowness population, we convert the dispersion curve in Figure 1(a) into a histogram as shown in Figure 1(b). A characteristic of dipole-flexural mode dispersion is that the slowness behaves as monotonic function of frequency. The dispersion curve usually flattens out at

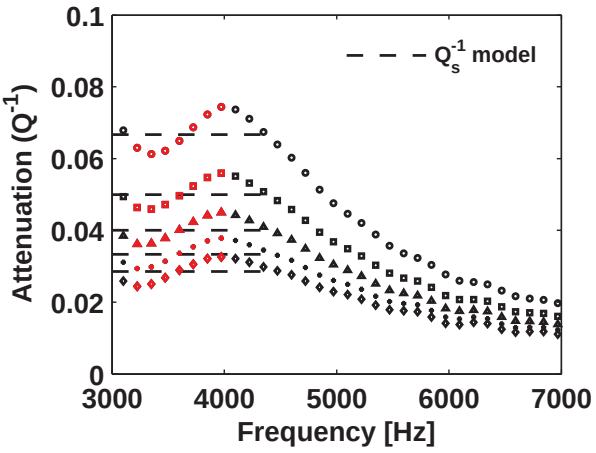

Figure 2: Synthetic data example: estimate formation shear attenuation from dipole-flexural wave attenuation. Different symbols denote different shear wave attenuation employed in the modeling.

low frequencies, where the flexural slowness approaches to the formation shear slowness asymptotically. This feature would lead to a local maximum in the histogram at the slowness values around the formation shear slowness. In Figure 1(b), the histogram indicates a formation shear slowness of 131 μs/ft which is within 1% of the actual value.

More importantly, the slowness probability analysis allows us to determine the frequency components that correspond to the formation shear slowness. For example in Figure 1(b), the histogram reveals that there are 23 frequencies at which the formation shear slowness are sampled. These frequency components may not be continuous depending on the flatness of the slowness at low frequencies. However, as an approximation, we can sample the smallest and the largest values from these 23 frequencies. Thus, a characteristic frequency range where the formation shear mode is dominant can be determined. The slownesses within this frequency band are plotted as red circles in Figure 1(a). It can be seen that this band is indeed within the flat portion of the dispersion curve.

Unlike the shear slowness at low frequencies, the flat portion of the attenuation is less evident. Therefore, direct application of the histogram method for determining the shear attenuation from the flexural attenuation curve becomes unstable. Instead, we can refer to the low frequency band pre-determined from the slowness probability analysis. We can then take the mean value of the attenuation within this band as an approximation for the formation shear attenuation. As the shear wave is dominating within this band, the attenuation would be close to the formation shear attenuation. In Figure 2, the attenuation components within the shear wave band is colored by red and their mean value is plotted as dashed line. We can see there is a good match between the model and the estimate. The deduced formation shear attenuation is within 1% of its actual value.

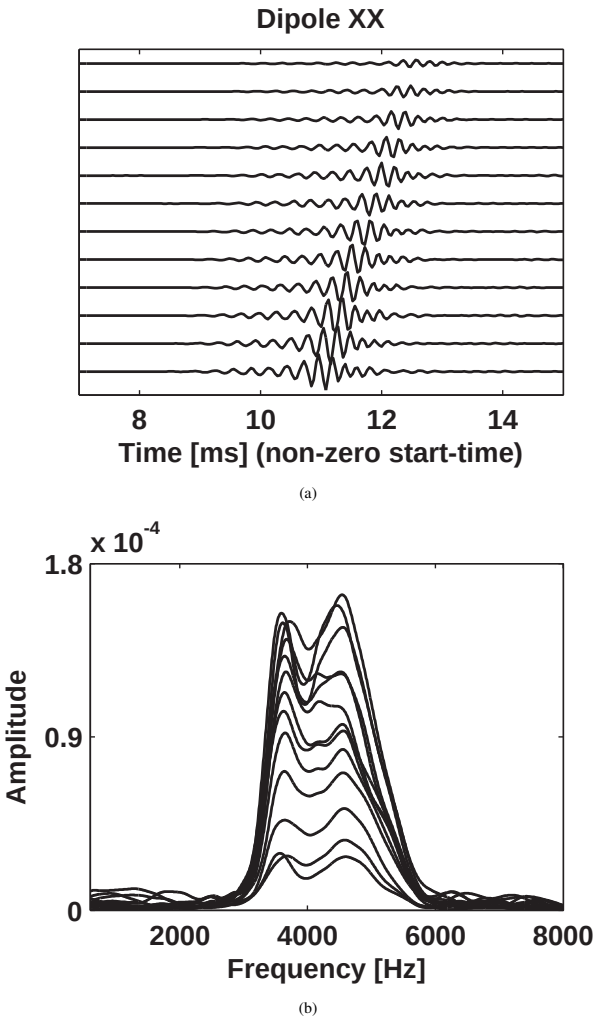

Figure 3: (a) Array dipole waveforms; (b) corresponding amplitude spectra.

FIELD DATA EXAMPLE

In this section, we apply the workflow on a test well data set. The full waveform dipole log is acquired by Halliburton sonic logging tool. The tool includes a receiver-array section which spans 6 ft long with 13 rings of hydrophone receivers. There are two broadband dipole sources (DX and DY) in the transmitter section. The waveforms recorded by the in-line XX transmitter-receiver array are displayed in Figure 3(a).. Corresponding amplitude spectra are plotted in Figure 3(b). The relative decay between the amplitude spectra with increasing travel distance is evident. This is desired for a reliable attenuation estimate. Figure 4(a) shows the slowness dispersion curve. The monotonic feature of the slowness is distinct and the flat portion of the dispersion curve can be visually identified. We conduct the slowness probability analysis in a histogram fashion to determine the formation shear slowness and the characteristic frequency band. In Figure 4(b), the histogram indicates a formation shear slowness of 142 μs/ft and a shear

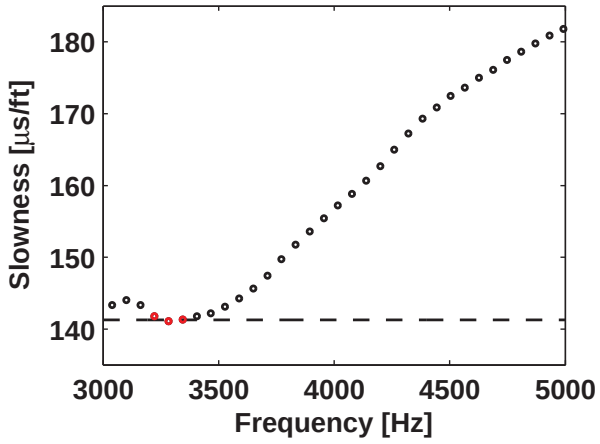

(a)

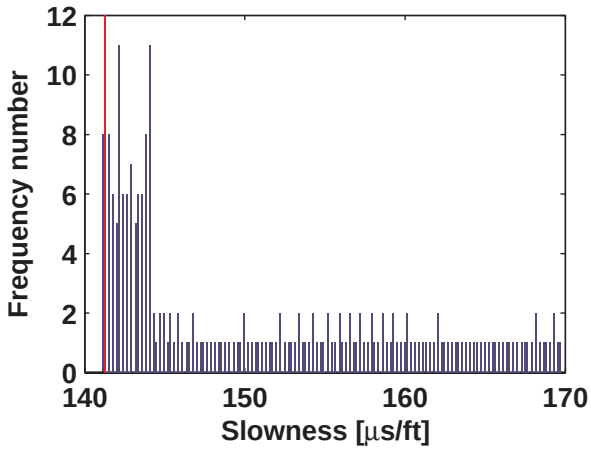

(b)

Figure 4: Field data example: (a) slowness dispersion; (b) slowness probability histogram.

wave band between 3.23-3.35 kHz. In Figure 5, the flexural wave attenuation exhibits a strong frequency dependency between 3 and 5 kHz. The inverse quality factor starts at 0.09 at high frequency and increases to a maximum value of 0.178 at low frequency. With decreasing frequency, the attenuation and slowness start to flatten at nearly the same frequency around 3.35 kHz, which conforms with our previous assumption. We calculate the formation shear attenuation by applying the characteristic band method. The result is given by the dashed line in Figure 5. The deduced formation shear attenuation matches with the asymptote of the flexural wave attenuation at low frequencies. Given the fact that flexural wave attenuation can be strongly frequency dependent, one should be cautious to apply constant-Q-based methods for estimating shear attenuation from dipole. Methods such as spectral ratio and centroid frequency shift would mix the effects of shear and mud attenuations. As a result, they would lead to biased Q_s estimate, particularly in fast formation.

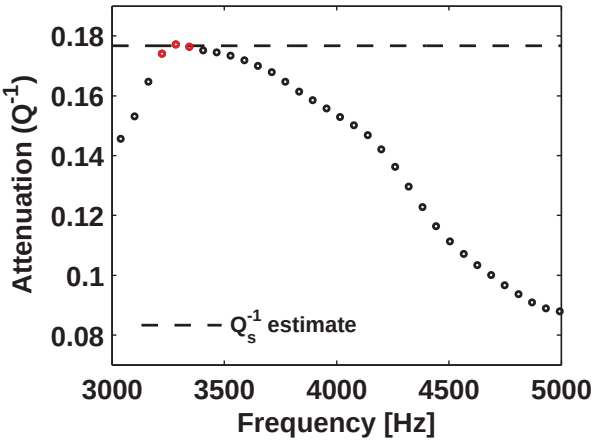

Figure 5: Field data example: estimate formation shear attenuation from dipole-flexural wave attenuation.

DISCUSSION

With an appropriate modification, the frequency-dependent attenuation analysis can also be applied to other borehole dispersive wave modes, such as Stoneley waves. Decoding the frequency-dependent attenuation and slowness of Stoneley wave provides a more controlled measure on the formation permeability. This serves as one of our future interests. In the current study, dipole attenuation estimate is only carried out for one component of the dipole data, that is, the waveforms recorded by the in-line XX transmitter-receiver array. Shear attenuation obtained from full 4-component cross-dipole data is potentially useful for formation fracture detection. Shear attenuation when applied together with compressional wave attenuation is another effective tool for hydrocarbon detection. All of these applications rely on the quality of the sonic waveform data and the robustness of the attenuation extraction method.

CONCLUSIONS

We extend the workflow of extracting dipole shear slowness to include estimation of formation shear attenuation. The method employs a low frequency band calibrated from the shear slowness probability to characterize the shear attenuation from the frequency-dependent flexural waves. The test results from the synthetic and real data validate the practical applicability of the proposed workflow. Our work suggests that accounting for the frequency dependency of flexural wave is important for accurately determining shear attenuation from dipole sonic logs.

ACKNOWLEDGMENTS

We acknowledge the EDB Petroleum Engineering Professorship for financial support. Dr. Yunyue Elita Li is funded by MOE Tier-1 Grant R-302-000-165-133.

REFERENCES

Cheng, C. H. A., M. N. Toksöz, and M. E. Willis, 1982, Determination of in situ attenuation from full waveform acoustic logs: Journal of Geophysical Research: Solid Earth, **87**, 5477–5484.

Huang, X., and H. Yin, 2005, A data-driven approach to extract shear and compressional slowness from dispersive waveform data, *in* SEG Technical Program Expanded Abstracts 2005: Society of Exploration Geophysicists, 384–387.

Li, Y., Y. Shen, and P. Kang, 2015, Integration of seismic and fluid-flow data: a two-way road linked by rock physics: Presented at the 77th EAGE Conference and Exhibition 2015.

Nolte, B., R. Rao, and X. Huang, 1997, Dispersion analysis of split flexural waves: Technical report, Massachusetts Institute of Technology. Earth Resources Laboratory.

Qi, Q., T. M. Müller, and M. Pervukhina, 2017, Sonic Q_p/Q_s ratio as diagnostic tool for shale gas saturation: Geophysics, **82**, in press.

Quan, Y., and J. M. Harris, 1997, Seismic attenuation tomography using the frequency shift method: Geophysics, **62**, 895–905.

Schmitt, D., 1988, Shear wave logging in elastic formations: The Journal of the Acoustical Society of America, **84**, 2215–2229.

Tang, X.-M., and C. H. A. Cheng, 2004, Quantitative borehole acoustic methods: Gulf Professional Publishing, **24**.